Entropy–Stabilized Metal Oxide Solid Solutions as CO Oxidation Catalysts with High–Temperature Stability

Hao Chen[1,3], Jie Fu[3], Pengfei Zhang[1], Honggen Peng[d,e], Carter W. Abney[2], Kecheng Jie[1], Xiaoming Liu[4], Miaofang Chi[4], Sheng Dai[1,2*]" should be "Hao Chen[a,c], Jie Fu[c], Pengfei Zhang[a], Honggen Peng[d,e], Carter W. Abney[b], Kecheng Jie[a], Xiaoming Liu[d], Miaofang Chi[d], Sheng Dai[a,b*]

[a] Department of Chemistry, The University of Tennessee, Knoxville, TN, 37996, USA

[b] Oak Ridge National Laboratory, Oak Ridge, TN 37831, USA

[c] Key Laboratory of Biomass Chemical Engineering of Ministry of Education, College of Chemical and Biological Engineering, Zhejiang University, Hangzhou, 310027, China

[d] Center for Nanophase Materials Sciences, Oak Ridge National Laboratory, Oak Ridge, TN, 37831, USA

[e] College of Chemistry, Nanchang University, 999 Xuefu Road, Nanchang, Jiangxi 330031, China

Corresponding Author: Sheng Dai, E-mail: dais@ornl.gov.

Experimental

Materials and Chemicals

$H_2PtCl_6 \cdot xH_2O$ (99.9%, ALDRICH, USA), $MgCl_2 \cdot 6H_2O$ (AR, ACROS, USA), $ZnCl_2$ (98%+, Alfa Aesar, USA), $CoCl_2$ (97.0%, ACROS, USA), $CuCl_2$ (AR, ACROS, USA) and $Ni(OOCCH_3)_2 \cdot 4H_2O$ (99.0%, ACROS, USA) were purchased as received. Ammonium hydroxide ($NH_3 \cdot H_2O$, 28.0~30.0%) was brought from Avantor Performance Materials (USA) and cetyltrimethyl ammonium bromide (CTAB, AR) was purchased from MP Biomedicals, LLC (France).

Synthesis of entropy-stabilized metal oxide solid solutions

NiMgCuZnCoOx (mix)

$MgCl_2 \cdot 6H_2O$, $ZnCl_2$, $CoCl_2$, $CuCl_2$ and $Ni(OOCCH_3)_2 \cdot 4H_2O$ are massed and physical mixed just using agate mortar. To ensure adequate mixing, all batches are milled for at least 2 h. Mixed powders are then calcinated in air under 800, 900 and 1000 °C for 4 h (5 °C/min) to obtain desired crystallineoxide phase.

NiMgCuZnCoOx (co-precipitation)

Equal molar ratio (0.02 M) of $MgCl_2 \cdot 6H_2O$, $ZnCl_2$, $CoCl_2$, $CuCl_2$ and $Ni(OOCCH_3)_2$ are dissolved in 30 ml water followed by adding the 0.47 g CTAB. After stirring for 12 h at 60 °C, 2.5 ml $NH_3 \cdot H_2O$ was added and continues stirring for 12 h at 60 °C. After filtering, the precipitatewas dried at 120 ◦C for 4 h and finally calcined at 900 ◦C for 4 h (5 °C/min)

to obtain desired crystallineoxide phase.

PtNiMgCuZnCoOx (co-deposition)

Equal molar ratio (0.02 M) of $MgCl_2 \cdot 6H_2O$, $ZnCl_2$, $CoCl_2$, $CuCl_2$ and $Ni(OOCCH_3)_2$ are dissolved in 30 ml water followed by adding the 0.47 g CTAB. After stirring for 12 h at 60 °C, precalculated amount of H_2PtCl_6 (0.3, 0.6 and 1.0 wt%) in H_2O was added and then stirred constantly for 12 h. 2.5 ml $NH_3 \cdot H_2O$ was added and continues stirring for 12 h at 60 °C. After filtering, the precipitatewas dried at 120 °C for 4 h and finally calcined at 900 ◦C for 4 h (5 °C/min) to obtain desired crystallineoxide phase.

The reduced 0.3wt%PtNiMgCuZnCoOx were measured under 300 °C for 2 h using a mixture of 4% H_2 in 96% N_2.

Characterization of the catalysts

The powder X-ray diffraction (XRD) data were recorded with a PANalytical Empyrean diffractometer, operated at 45 kV and 40 mA (scanning step: 0.02 ° per step). The diffraction patterns were recorded in the range of 10-80°. The nanoparticle size (dBa, nm) was estimated according to Scherrer equation: S4 dBa = K·λ/(β· cosθ) (K = 0.9, λ = 0.1540598 nm).

The nitrogen adsorption and desorption isotherms were measured at 77 K under a Gemini VII surface area analyzer. Samples were degassed for 12 h under N_2 at 100 ℃ prior to the measurement.

High resolution transmission electron microscopy (HRTEM) and high-angle annular dark-field scanning transmission electron microscopy (HAADF-STEM) were conducted on

an aberration-corrected FEI Titan S 80-300 TEM/STEM operated at 300 kV and a large active area (60mm2) EDAX silicon drift detector (SDD) for high-collection-efficiency energy dispersive x-ray spectroscopy (EDS).

X-ray photoelectron spectroscopy (XPS) experiments were performed with a PHI 3056 spectrometer equipped with an Al anode source operated at 15 KV and an applied power of 350 W and a pass energy of 93.5 eV.

X-ray photoelectron spectroscopy (XPS) were performed with a PHI 3056 spectrometer equipped with an Al anode source operated at 15 KV and an applied power of 350 W and a pass energy of 93.5 eV.

Temperature-programmed reduction of H_2 (H_2-TPR) experiments were conducted on a PX200 apparatus with a TCD. 50 mg of sample was pretreated at 450 °C (10 °C/min) in He for 1 h and then cooled to room temperature. Then the sample was directly heated from 60 °C to 700 °C at a rate of 10 °C/min in a flow of 5 vol % H_2/N_2 (40 mL/min). The hydrogen consumption was quantitatively evaluated by the TCD signal.

Catalytic CO oxidation

Catalytic CO oxidation was carried out in a fixed-bed reactor (straight quartz tube) at atmospheric pressure [1]. For the measurement of CO light-off curves showing CO conversion as a function of reaction temperature, a 20 mg catalyst supported by quartz wool was loaded in the reactor. The feed gas of 1 % CO balanced with dry air (< 4 ppm water) passed though the catalyst bed at a flow rate of 10 ml/min corresponding to gas hourly space velocity (GHSV) of 30,000 mL (h g_{cat})$^{-1}$. The concentrations of CO and CO_2 in the

reactor effluent were analyzed by a Buck Scientific 910 gas chromatograph equipped with a dual molecular sieve/porous polymer column (Alltech CTR1) and a thermal conductivity detector. We controlled the reaction temperature through changing its discharge and maintained at each temperature point for 5 min to detect each experiment for two times.
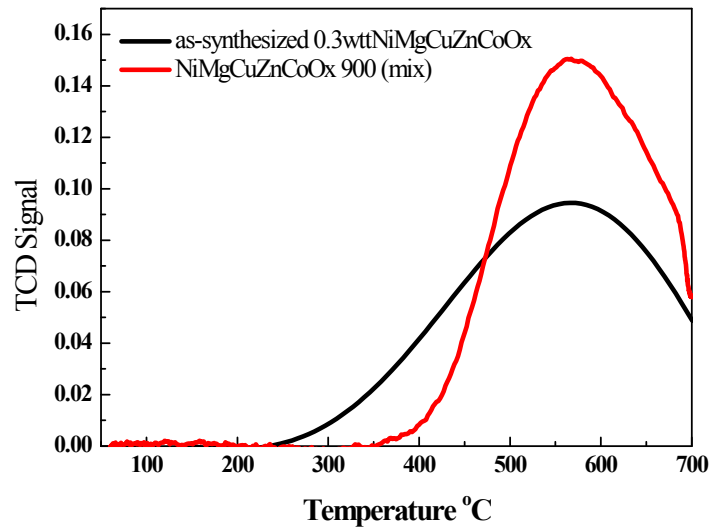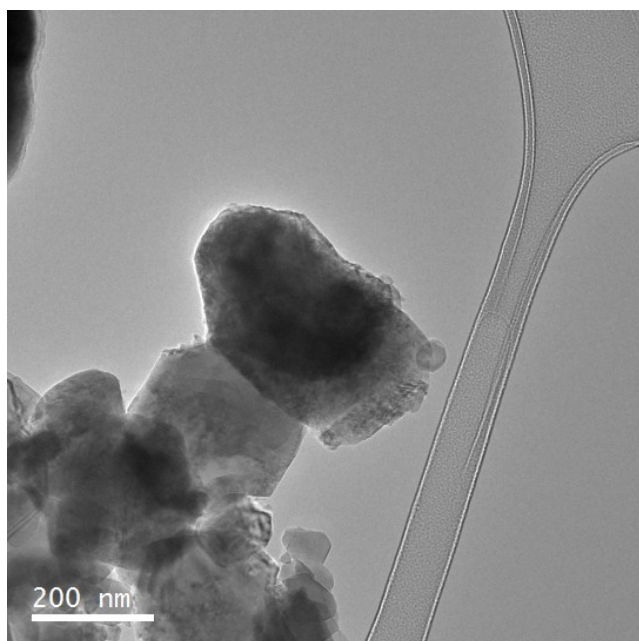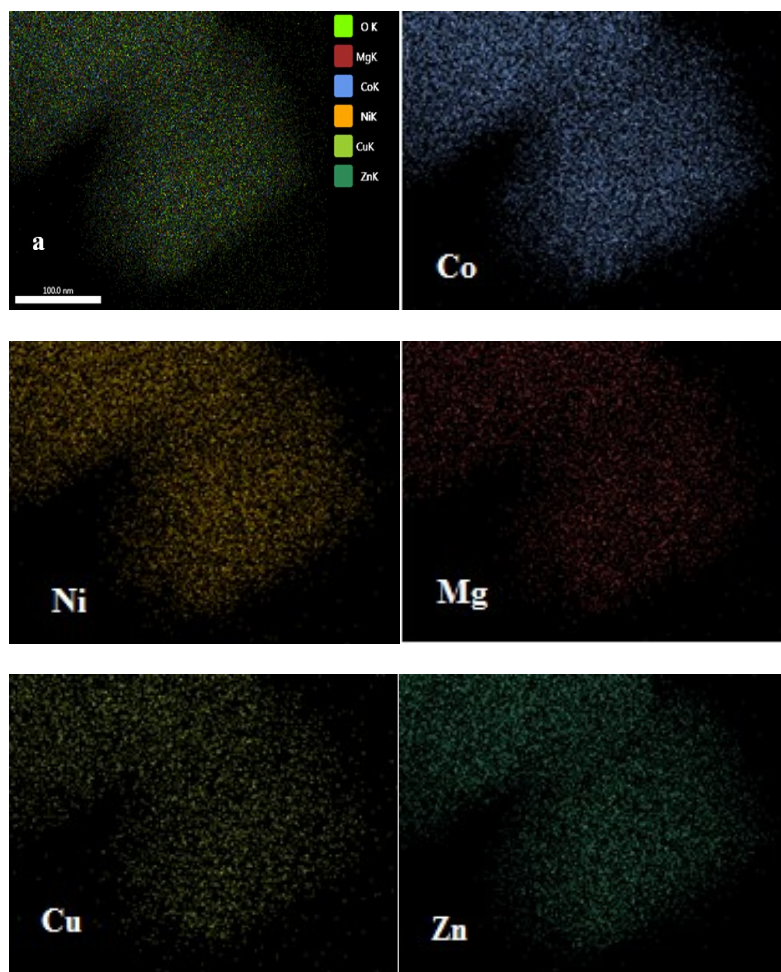
Figure S1. TPR result of NiMgCuZnCoO$_x$ 900 and as–synthesized

0.3wt%PtNiMgCuZnCoO$_x$.
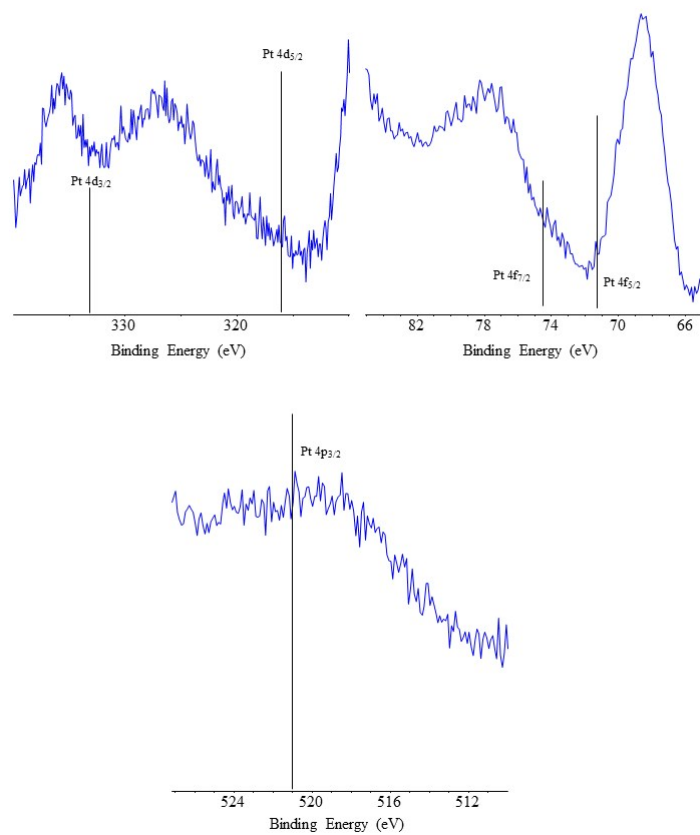
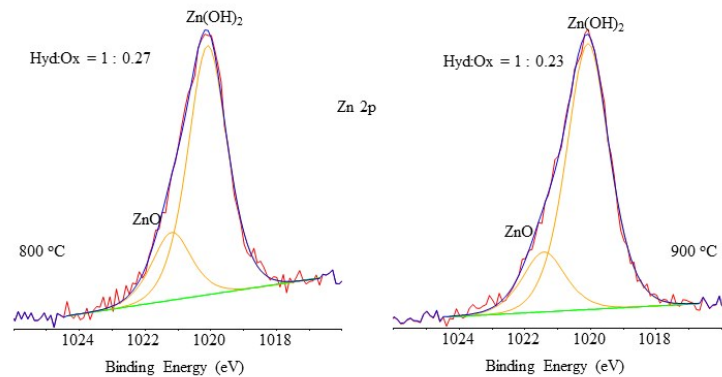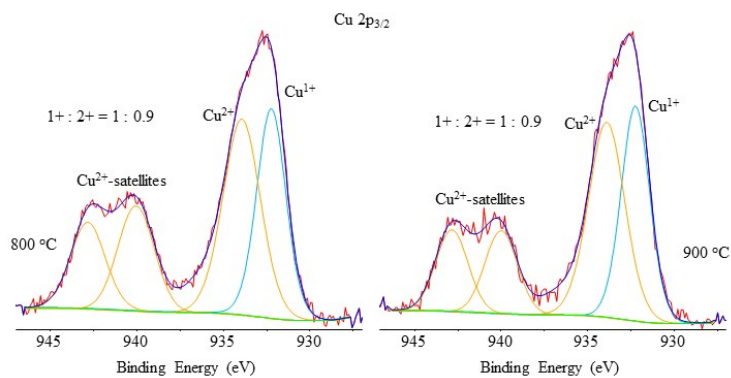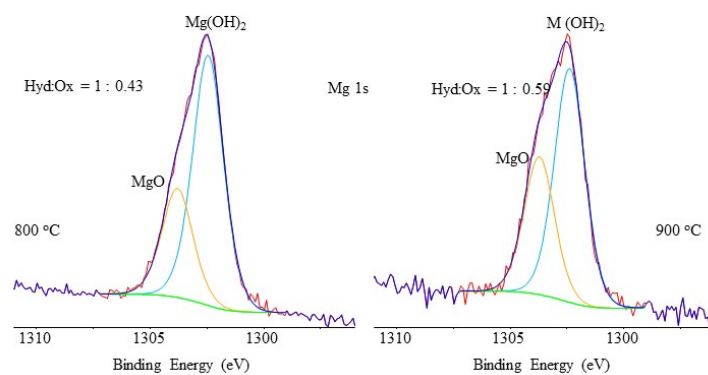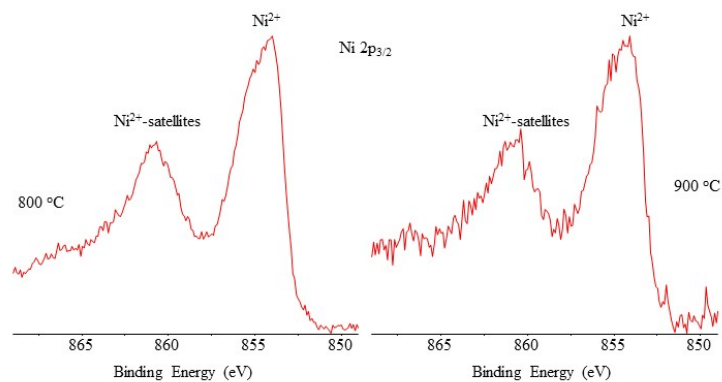**Figure S2.** HRTEM images of reduced $0.3wt\%PtNiMgCuZnCoO_x$.

Figure S3. TEM–EDS analysis of reduced 0.3wt%PtNiMgCuZnCoO$_x$.

Figure S4. XPS results of Pt in reduced 0.3wt%PtNiMgCuZnCoO$_x$.

Ni 2p$_{3/2}$

Ni^{2+}

Ni^{2+}-satellites

800 °C

Ni^{2+}

Ni^{2+}-satellites

900 °C

865 860 855 850
Binding Energy (eV)

865 860 855 850
Binding Energy (eV)

Mg 1s

Mg(OH)$_2$

Hyd:Ox = 1 : 0.43

MgO

800 °C

M (OH)$_2$

Hyd:Ox = 1 : 0.59

MgO

900 °C

1310 1305 1300
Binding Energy (eV)

1310 1305 1300
Binding Energy (eV)

Cu 2p$_{3/2}$

1+ : 2+ = 1 : 0.9

Cu^{2+}

Cu^{1+}

Cu^{2+}-satellites

800 °C

1+ : 2+ = 1 : 0.9

Cu^{2+}

Cu^{1+}

Cu^{2+}-satellites

900 °C

945 940 935 930
Binding Energy (eV)

945 940 935 930
Binding Energy (eV)

Zn 2p

Zn(OH)$_2$

Hyd:Ox = 1 : 0.27

ZnO

800 °C

Zn(OH)$_2$

Hyd:Ox = 1 : 0.23

ZnO

900 °C

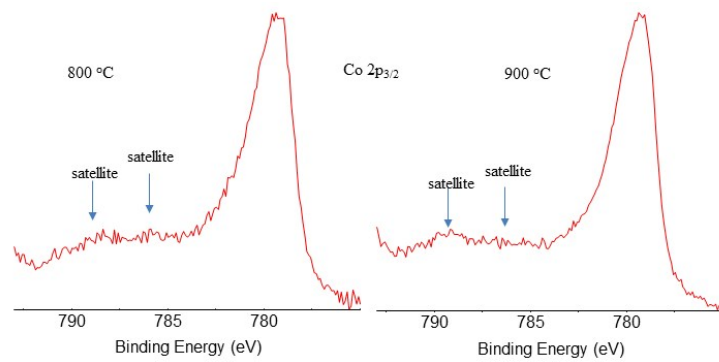1024 1022 1020 1018
Binding Energy (eV)

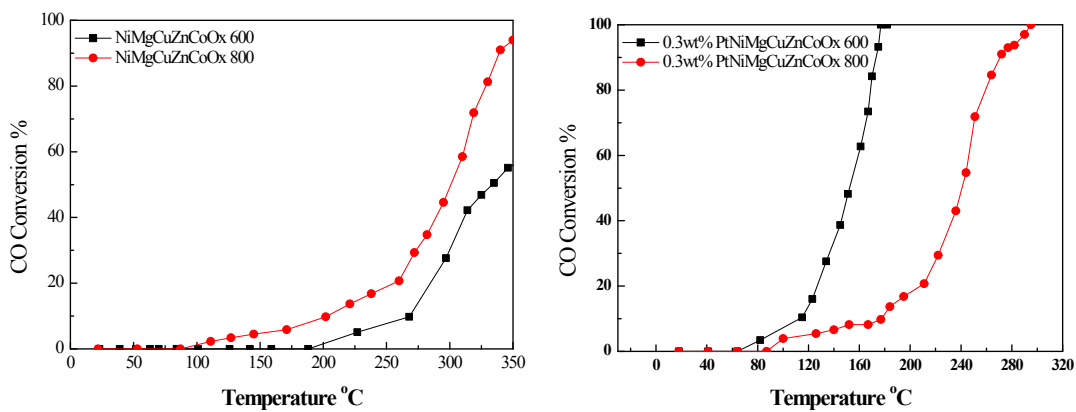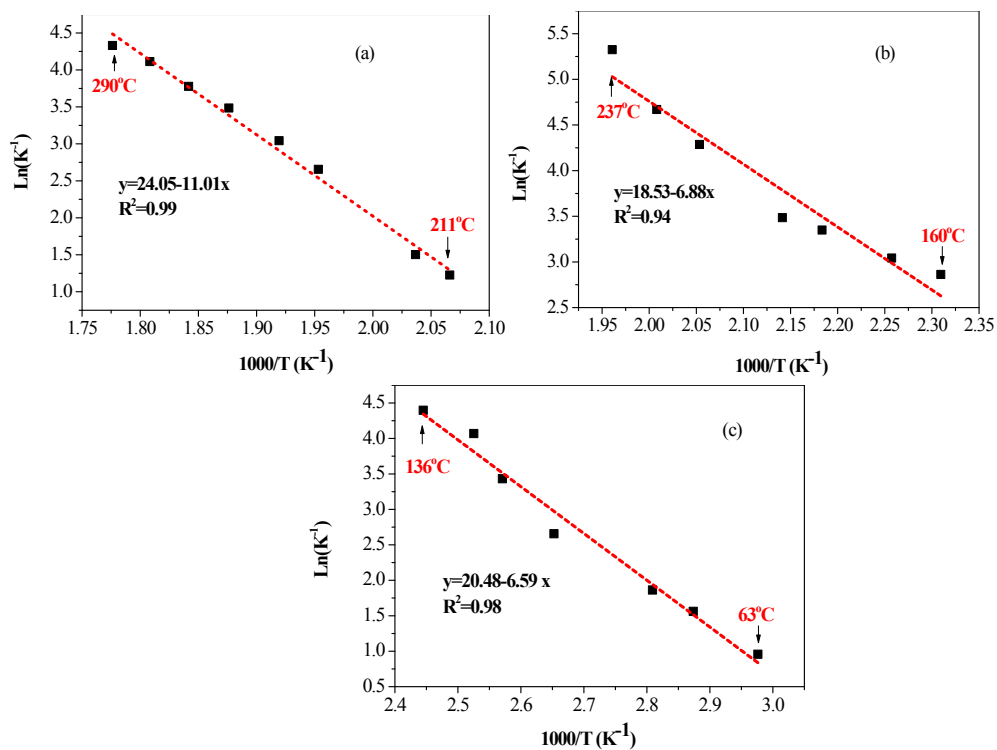1024 1022 1020 1018
Binding Energy (eV)

S10

Figure S5. XPS results of Ni, Mg Cu, Zn and Co in NiMgCuZnCoO$_x$ treated at 800 °C and 900 °C.
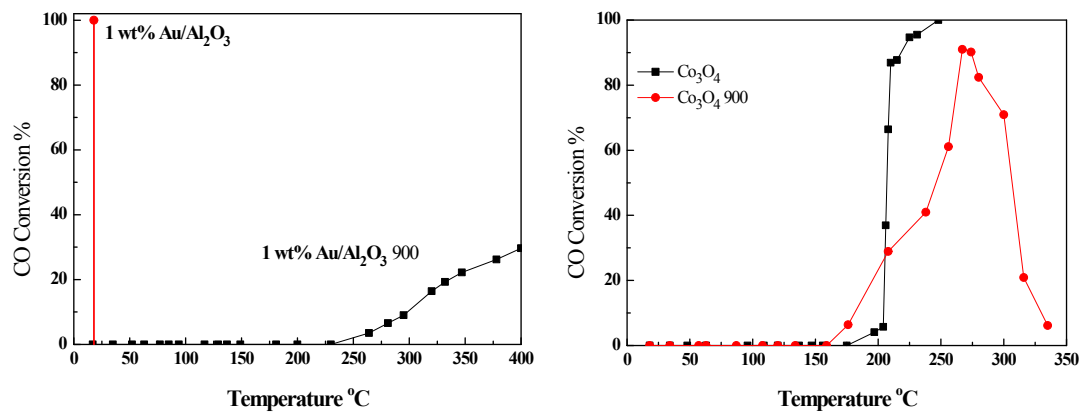
Figure S6. CO oxidation over NiMgCuZnCoO$_x$ and reduced 0.3wt%PtNiMgCuZnCoO$_x$ calcined at 600 and 800 ^{o}C.

Figure S7. The variation of Lnk with the 1/T for (a) NiMgCuZnCoO$_x$ 900; (b) as–synthesized 0.3wt%PtNiMgCuZnCoO$_x$ and (c) reduced 0.3wt%PtNiMgCuZnCoO$_x$. The relations between Lnk and 1/T were all found to be in linearly.
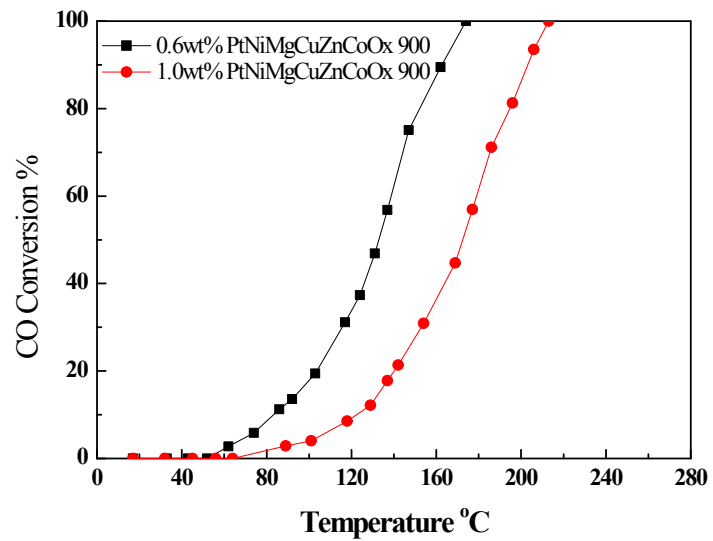
Figure S8. CO oxidation over reduced PtNiMgCuZnCoO$_x$ 900 with different Pt loading.

Figure S9. CO oxidation over 1wt%Au/Al$_2$O$_3$ and Co$_3$O$_4$ (as–received and calculated at 900 ^{o}C).

Table S1. Calculated pre–exponential factor (A) and apparent activation energy (Eα) for NiMgCuZnCoO$_x$ 900, as–synthesized 0.3wt%PtNiMgCuZnCoO$_x$ and reduced 0.3wt%PtNiMgCuZnCoO$_x$.

Catalyst	A (min^{-1})	E_a (KJ·mol^{-1})
NiMgCuZnCoO$_x$ 900	2.78×10^{10}	91.5±3.57
as–synthesized 0.3wt%PtNiMgCuZnCoO$_x$	1.12×10^8	57.2±6.07
reduced 0.3wt%PtNiMgCuZnCoO$_x$	7.53×10^8	54.8±3.41

References:

1. C. Tian, X. Zhu, C. W. Abney, X. Liu, G. S. Foo, Z. Wu, M. Li, H. M. Meyer, S. Brown, S. M. Mahurin, S. Wu, S. Z. Yang, J. Liu and S. Dai, ACS Catal., 2017, 7, 3388–3393.